Am. J. Hum. Genet. 74:1255–1261, 2004

Report

The Novel Gene Encoding a Putative Transmembrane Protein Is Mutated in Gnathodiaphyseal Dysplasia (GDD)

Satoshi Tsutsumi,[1,2] Nobuyuki Kamata,[1] Tamara J. Vokes,[3] Yutaka Maruoka,[4] Koichi Nakakuki,[5] Shoji Enomoto,[4] Ken Omura,[4] Teruo Amagasa,[5] Masaru Nagayama,[1] Fumiko Saito-Ohara,[6] Johji Inazawa,[6] Maki Moritani,[2] Takashi Yamaoka,[2] Hiroshi Inoue,[2] and Mitsuo Itakura[2]

[1]First Department of Oral and Maxillofacial Surgery, School of Dentistry, and [2]Division of Genetic Information, Institute for Genome Research, University of Tokushima, Tokushima, Japan; [3]Section of Endocrinology, Department of Medicine, University of Chicago, Chicago; and [4]Section of Oral Surgery, Department of Oral Restitution, Division of Oral Health Sciences, [5]Section of Maxillofacial Surgery, Graduate School, and [6]Department of Molecular Cytogenetics, Medical Research Institute, Tokyo Medical and Dental University, Tokyo

Gnathodiaphyseal dysplasia (GDD) is a rare skeletal syndrome characterized by bone fragility, sclerosis of tubular bones, and cemento-osseous lesions of the jawbone. By linkage analysis of a large Japanese family with GDD, we previously mapped the GDD locus to chromosome 11p14.3-15.1. In the critical region determined by recombination mapping, we identified a novel gene (*GDD1*) that encodes a 913-amino-acid protein containing eight putative transmembrane-spanning domains. Two missense mutations (C356R and C356G) of *GDD1* were identified in the two families with GDD (the original Japanese family and a new African American family), and both missense mutations occur at the cysteine residue at amino acid 356, which is evolutionarily conserved among human, mouse, zebrafish, fruit fly, and mosquito. Cellular localization to the endoplasmic reticulum suggests a role for GDD1 in the regulation of intracellular calcium homeostasis.

In 1969, Akasaka et al. described a large Japanese family including 21 patients exhibiting frequent bone fractures in adolescence and purulent osteomyelitis of the jaws during adult life, with autosomal dominant inheritance. In this family, patients experienced frequent bone fractures caused by trivial accidents in childhood; however, the fractures healed normally without bone deformity. The jaw lesions in patients replace the tooth-bearing segments of the maxilla and mandible with fibrous connective tissues, including various amounts of cementum-like calcified mass, sometimes causing facial deformities (fig. 1*A* and 1*B*). Patients also have a propensity for jaw infection and often suffer from purulent osteomyelitis-like symptoms, such as swelling of and pus discharge from the gums, mobility of the teeth, insufficient healing after tooth extraction, and exposure of the lesions into the oral cavity. Extragnathic skeletal changes consist of generalized coarse bony trabeculae and gross thickening of the diaphyseal cortices of long bones (fig. 1*C* and 1*D*). This syndrome was named "hereditary gnatho-diaphyseal sclerosis" (Akasaka et al. 1969), because it was distinguished from known systemic bone diseases by coincidence of bone fragility, sclerosis of tubular bones, cemento-osseous lesions of the jawbone, and no abnormality in nonskeletal tissues. In 1985, Levin et al. independently described three families—whose condition shared many features with that reported by Akasaka et al.—as having "osteogenesis imperfecta with unusual skeletal lesions" (MIM 166260) (Levin et al. 1985). Sporadic cases with similar clinical manifestations have also been reported (Colavita et al. 1984; Nishimura et al. 1996). More recently, Riminucci et al. proposed to name this disease entity "gnathodiaphyseal dysplasia (GDD)," because osteosclerosis is not a feature of the jaw lesions of these patients (Riminucci et al. 2001).

By linkage analysis of the Japanese family reported by Akasaka et al., we previously mapped the GDD locus to a 8.7-cM interval on chromosome 11p14.3-15.1, flanked by the recombinant markers D11S1308 and

Received January 9, 2004; accepted for publication March 17, 2004; electronically published April 29, 2004.

Address for correspondence and reprints: Dr. Nobuyuki Kamata, Department of Oral and Maxillofacial Surgery, Division of Cervico-Gnathostomatology, Graduate School of Biomedical Sciences, Hiroshima University, Kasumi 1-2-3, Minami-ku, Hiroshima 734-8553, Japan. E-mail: nokam@hiroshima-u.ac.jp

0002-9297/2004/7406-0019$15.00

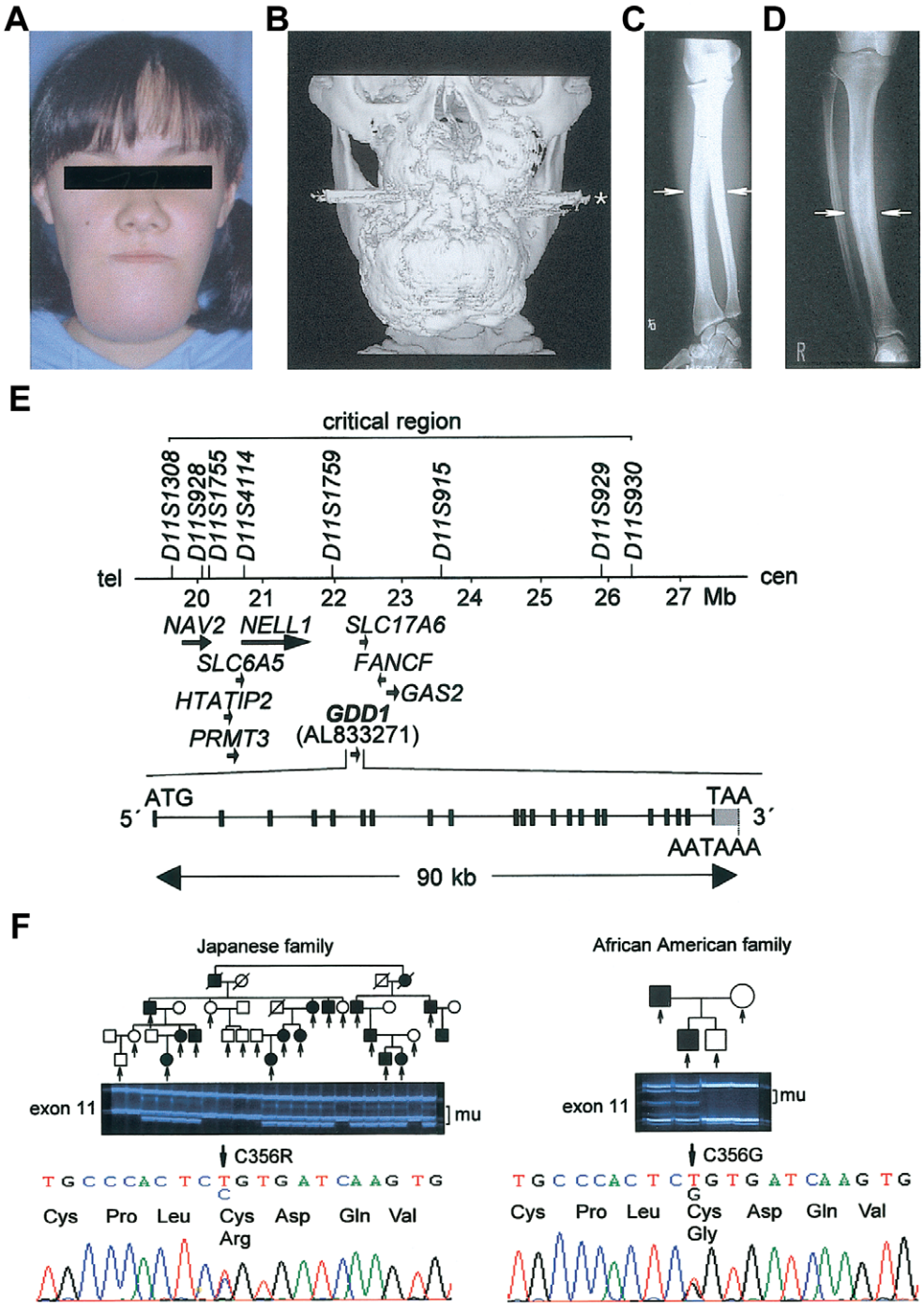

Figure 1 GDD phenotype and mutations. *A*, Affected female from Japanese family at age 16 years; facial deformity characteristic of the GDD phenotype is shown. *B*, Three-dimensional image of computed tomography. The image shows jaw lesions occupying alveolar processes. Projections around teeth (*asterisk*) are metal artifacts caused by teeth fillings. *C, D*, Radiographs of upper and lower limbs showing diaphyseal cortical thickening of tubular bones (*arrows*). *E*, Physical map of the GDD critical region and genomic structure of *GDD1*. Exons (*filled boxes*) and UTRs (*gray box*) are shown. *F*, Sequence analysis showing heterozygous T-to-C and T-to-G changes in the codon for Cys^{356} in affected members of the Japanese and African American families, respectively. SSCP patterns show cosegregation of mutant alleles (mu) with the disease phenotype. Individuals available for analyses are indicated (*arrows*).

D11S930, where no bone-disease loci have been mapped (Tsutsumi et al. 2003). On the basis of data from the University of California–Santa Cruz (UCSC) genome browser (UCSC Genome Bioinformatics Web site), the GDD critical region was shown to contain eight known genes (*NAV2, HTATIP2, PRMT3, SLC6A5, NELL1, SLC17A6, FANCF,* and *GAS2*) (fig. 1*E*). By use of DNA samples from the Japanese family, these genes were screened for mutations by direct DNA sequencing with primer pairs that amplified all exons and exon-intron boundaries, but no mutations were detected.

In a further search for GDD candidate genes, we prioritized uncharacterized ESTs (expressed sequence tag sequences) that mapped to the critical region. A cDNA clone sequence AL833271 from skeletal muscle had a size of ~6.7 kb, exhibited the polyadenylation signal (AATAAA) at the 3′ end, and included an ORF of 2,742 bp encoding a protein of 913 amino acids, with a molecular mass of 107.20 kDa. A human skeletal muscle cDNA was amplified by 5′ rapid amplification of cDNA ends (RACE) (Invitrogen), revealing that AL833271 was a full-length cDNA sequence. We named this gene "*GDD1*" (GenBank accession number AB125267). Aligning the UCSC July 2003 human genome assembly (UCSC Genome Bioinformatics Web site) with AL833271 revealed that *GDD1* consisted of 22 exons and spanned ~90 kb of genomic DNA (fig. 1*E*). The initiation and stop codons (ATG and TAA) were present in exons 1 and 22, respectively.

Oligonucleotide primers were designed to amplify and directly sequence the 22 exons, along with the flanking exon-intron boundaries (table A1 [online only]). Screening DNA from the Japanese family revealed that 14 affected members were heterozygous for a missense mutation in exon 11 at codon 356 (C356R; TGT→CGT), whereas 8 unaffected members had no mutation. Also, DNA sequencing in two affected members, but not in two unaffected members, from a new family of African American origin with GDD revealed another missense mutation at the same codon 356 (C356G; TGT→GGT). SSCP analysis confirmed that mutant alleles of *GDD1* cosegregated with the disease phenotype in each family (fig. 1*F*). Neither of these two mutations was found in 488 Japanese or 80 African American control individuals.

The GDD1 protein showed no significant similarity to any other known protein or protein classes. However, amino acid sequence analysis using the helix-prediction program TMpred suggested that GDD1 contains eight transmembrane-spanning domains, with the N- and C-termini located in the cytosol (fig. 2*A* and 2*B*). MOTIF and PSORT II also predicted five putative N-glycosylation sites and a potential endoplasmic reticulum (ER) retention signal (Teasdale and Jackson 1996) at the C-terminus (AKST), respectively (fig. 2*C*). On the other hand, BLAST analysis showed potentially orthologous sequences in zebrafish, fruit fly, and mosquito, indicating that the GDD1 protein is evolutionarily conserved. Mouse *GDD1* (*mGDD1*) cDNA was isolated from mouse skeletal muscle cDNA (Clontech) and completed by RT-PCR by use of a mouse genome sequence with high homology to human *GDD1* (*hGDD1*), which was identified through Ensembl (Ensembl Genome Browser Web site). The protein predicted from *mGDD1* cDNA sequence shared 79% amino acid identity with the human GDD1 protein (hGDD1). Multiple sequence alignment of hGDD1 with its orthologs revealed that the eight cysteine residues at positions 342, 353, 356, 360, 369, 601, 606, and 804 in the putative extracellular loops were absolutely conserved in all species (fig. 2*C*). These cysteine residues are expected to play an important role in the formation of intrachain disulfide bonds that are crucial for an appropriate tertiary structure of the hGDD1 protein, and the mutations of C356R and C356G probably compromise the conformation (fig. 2*B*).

The pattern of tissue expression was determined by a 581-bp fragment corresponding to the 3′ UTR of *hGDD1* cDNA, hybridized to a human Multiple Tissue Northern Blot (Clontech). Two major transcripts of ~7.5 and ~4.5 kb were detected in skeletal muscle, heart, and pancreas (fig. 3*A*). Since affected tissues were not represented on this blot, we examined levels of *hGDD1* gene expression in explant cultures of normal human osteoblasts and periodontal ligament cells, as well as in nonskeletal tissues (Human Total RNA Master Panel [Clontech]), by RT-PCR analysis. Expression of *hGDD1* was detected in brain, heart, kidney, lung, and skeletal muscle at usual conditions (30 cycles) and was detectable after 40 cycles in explant cultures of osteoblasts and periodontal ligament cells, as well as the other tissues shown in figure 3*B*. Quantitative real-time RT-PCR analysis of various tissues derived from one mouse aged 8 wk revealed that *mGDD1* was highly expressed in bone tissues, such as calvaria, femur, and mandible (fig. 3*C*). Although this result appears to be in contrast with the low level of *hGDD1* gene expression in human osteoblasts, we believe that the discrepancy in expression level might arise from differences in the samples used (explant cultures after three or four passages versus fresh bone tissues). The expression profile in vivo could not be reproduced completely in explant cultures.

To search the potential impact of the identified mutations, we transfected COS-7 cells with a plasmid expression vector containing the wild-type or mutant full-length hGDD1 cDNA tagged with V5 epitope at its 3′ end. On reducing SDS-PAGE and western blot analysis, anti-V5 antibody detected a band migrating at ~110 kDa in the whole-cell lysate of each transfectant (fig. 4*A*). The band size was consistent with the predicted molec-

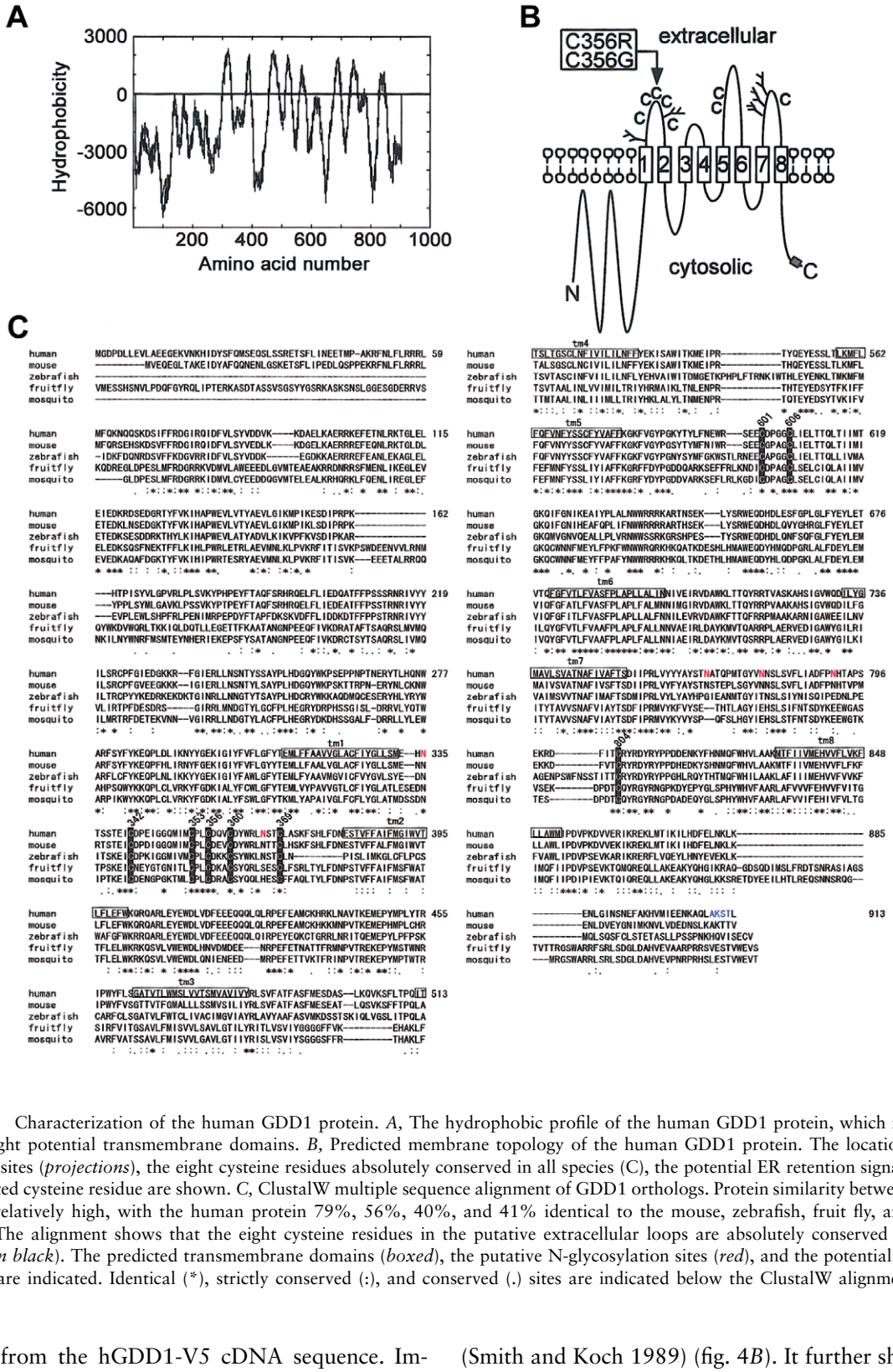

Figure 2 Characterization of the human GDD1 protein. *A*, The hydrophobic profile of the human GDD1 protein, which indicates that it contains eight potential transmembrane domains. *B*, Predicted membrane topology of the human GDD1 protein. The locations of the N-glycosylation sites (*projections*), the eight cysteine residues absolutely conserved in all species (C), the potential ER retention signal (*gray box*), and the mutated cysteine residue are shown. *C*, ClustalW multiple sequence alignment of GDD1 orthologs. Protein similarity between the GDD1 orthologs is relatively high, with the human protein 79%, 56%, 40%, and 41% identical to the mouse, zebrafish, fruit fly, and mosquito, respectively. The alignment shows that the eight cysteine residues in the putative extracellular loops are absolutely conserved in all species (*highlighted in black*). The predicted transmembrane domains (*boxed*), the putative N-glycosylation sites (*red*), and the potential ER retention signal (*blue*) are indicated. Identical (*), strictly conserved (:), and conserved (.) sites are indicated below the ClustalW alignment of GDD1 orthologs.

ular mass from the hGDD1-V5 cDNA sequence. Immunofluorescent staining of transfected cells with anti-V5 antibody showed that the wild-type hGDD1 protein formed a distinct reticular pattern around the nucleus and colocalized with calreticulin, an ER-specific marker (Smith and Koch 1989) (fig. 4*B*). It further showed that cells overexpressing each mutant hGDD1 protein, but not the wild-type hGDD1 protein, decreased cell adhesion and changed the cell morphology to a round shape (fig. 4*C*). However, these rounded cells showed

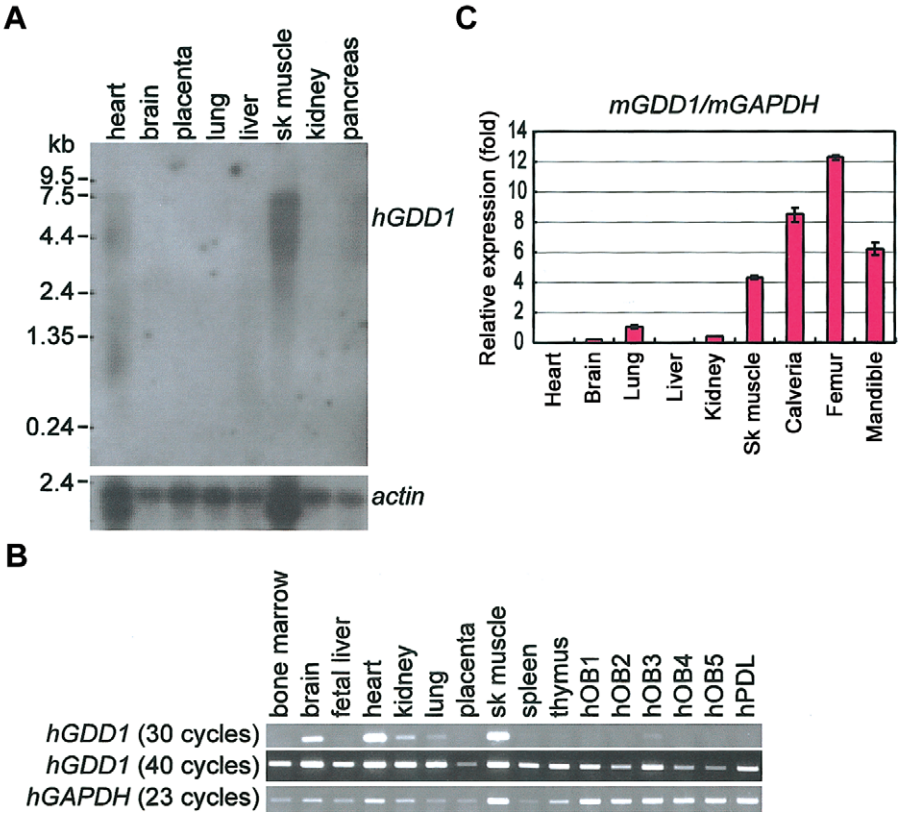

Figure 3 Expression analysis of *GDD1* mRNA in human and mouse tissues. *A*, A human Multiple Tissue Northern Blot (Clontech), hybridized with a ^{32}P-labeled 581-bp fragment of *hGDD1* cDNA (*upper panel*). The blot was rehybridized with ^{32}P-labeled *β-actin* cDNA as a loading control (*lower panel*). *B,* RT-PCR analysis for *hGDD1* mRNA in human tissues, normal human osteoblasts, and normal human periodontal ligament cells. We used osteoblasts isolated from jawbone specimens (hOB1–4) by use of the explant culture method (Hahn et al. 1988), osteoblasts from femur (hOB5 [Cambrex]), and periodontal ligament cells (hPDL) isolated from extracted tooth by use of the explant culture method. These cells were maintained in α-minimum essential medium containing 10% fetal bovine serum, 50 μg/ml of L-ascorbic acid, 50 U/ml penicillin, and 50 μg/ml streptomycin, and used at passage 3–4 for extraction of total RNA. A 348-bp fragment of *hGDD1* cDNA was amplified by use of primers from exons 9 and 12. PCR was performed by use of Platinum *Taq* (Invitrogen) at 95°C for 2 min, followed by 30 or 40 cycles of 94°C for 30 s, 55°C for 30 s, and 72°C for 30 s. A 452-bp fragment of *hGAPDH* cDNA was amplified as an internal control. *C,* Relative expression of *mGDD1* (normalized to *mGAPDH*) in mouse tissues. A real-time, two-step RT-PCR analysis was performed by use of SYBR Green PCR Master Mix (Applied Biosystems) and the ABI Prism 7900HT system (Applied Biosystems). Total RNA was isolated from various tissues of mouse aged 8 wk and reverse transcribed into random-primed first-strand cDNA. Specific PCR primer sets for *mGDD1* and *mGAPDH* were designed to avoid amplification of genomic DNA. The relative quantity was determined by the standard curve method, in which the standard curves were generated by 10-fold serial dilution of mouse skeletal muscle cDNA. The normalized values were derived from the ratio of the relative quantity of *mGDD1* for each sample to that of *mGAPDH* for that sample. Data are presented as the means ± SD of three independent experiments.

no features of apoptotic cell death, such as chromatin condensation or DNA fragmentation (data not shown).

In the present study, *GDD1* mutations were identified in two families with different genetic backgrounds who were both affected with GDD. We believe that mutant alleles at *GDD1* are responsible for the disease for several reasons, in addition to the fact that the gene maps to the critical region. In each of the two families, mutant alleles of *GDD1* cosegregated with the disease phenotype. Both missense mutations involved the cysteine residue at amino acid 356, which is evolutionarily conserved in human, mouse, zebrafish, fruit fly, and mosquito, further suggesting the biological significance of these mutations. None of the mutations was observed in normal chromosomes. *hGDD1* was shown to be expressed in human osteoblasts and periodontal ligament cells, consistent with the disease phenotype and the previous studies suggesting that cemento-osseous lesions of the jaws originate in the periodontal ligament (Waldron and Giansanti 1973; Neville and Albenesius 1986). In mouse, *mGDD1* mRNA was shown to be abundant in fresh bone tissues.

Although hGDD1 seemed to be an integral membrane protein localizing in the ER, its function remains unknown. As a clue to the function, membrane proteins localizing in the ER are often involved in protein pro-

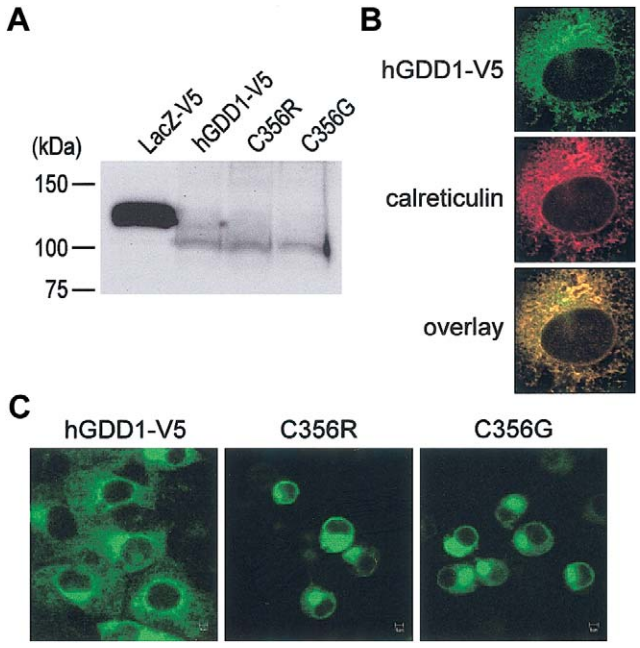

Figure 4 Expression of the hGDD1 protein in COS-7 cells. *A*, Western blot analysis to confirm expression of the wild-type and mutant hGDD1 proteins. Whole-cell lysates from COS-7 cells transfected with each plasmid expression vector containing the wild-type (hGDD1-V5) or mutant (C356R or C356G) hGDD1 cDNA tagged with V5 epitope at its 3′ end were subjected to reducing SDS-PAGE, and western blot analysis was performed by use of anti-V5 antibody (Invitrogen). For control transfection, pcDNA6/lacZ-V5 (Invitrogen) was used to represent the expression of an unrelated exogenous protein. *B*, Cellular localization of the wild-type hGDD1 protein. V5-tagged hGDD1 protein (hGDD1-V5) formed a distinct reticular pattern around the nucleus (*green*). Costaining with antibody against the calreticulin ER-specific marker (*red*) showed colocalization with the hGDD1 protein (*yellow*). *C*, Immunofluorescent staining with anti-V5 antibody, which shows that the only cells overexpressing each mutant hGDD1 protein decrease cell adhesion and change the cell morphology to a round shape.

cessing, protein folding, or calcium homeostasis. The amino acid sequence of hGDD1 lacks calcium or ATP-binding motifs and contains no homology to heat-shock proteins or GroEL, thereby providing no evidence for a direct involvement of hGDD1 in protein folding or calcium sequestration (Ma and Hendershot 2001). Instead, the presence of eight predicted transmembrane-spanning domains suggests that hGDD1 might function in the transport of ions or other small molecules across membranes. We speculate that hGDD1 might function as an intracellular calcium-release channel and that it might regulate a calcium-dependent signaling pathway. Various substances that influence bone remodeling modify the intracellular calcium concentration in osteoblasts (Meszaros and Karin 1995). There are two sources of intracellular calcium in osteoblasts: (1) inflow from the extracellular space and (2) release from intracellular stores, such as the ER. The release of calcium from the ER is a ubiquitous signal in many cells, including osteoblasts (Kumagai et al. 1991; Ljunggren et al. 1991). Given that each mutant hGDD1 induces excess calcium release from the ER, the alteration in cell shape (as described above) could occur through modulation of the cytoskeleton (Pettit and Fay 1998). Further studies of the function of hGDD1 should yield crucial insights into the pathogenesis of GDD.

Acknowledgments

We thank the patients with GDD and their families for their participation in this study. This study was approved by institutional review boards of the University of Tokushima and the University of Chicago. We thank Drs. David Ehrman and Graeme Bell for 50 African American control samples, derived from the General Clinical Research Center at the University of Chicago (grant M01RR00055). We also thank Dr. Takayuki Morisaki for 30 African American control samples. This work was supported by grants from the Ministry of Education, Culture, Sports, Science, and Technology of Japan (Special Coordination Funds for Promoting Science and Technology) and the Japan Society for the Promotion of Science (Research for the Future Program).

Electronic-Database Information

Accession numbers and URLs for data presented herein are as follows:

BLAST, http://www.ncbi.nlm.nih.gov/BLAST/
ClustalW, http://www.ddbj.nig.ac.jp/E-mail/homology.html
Ensembl Genome Browser, http://www.ensembl.org/Mus_musculus/ (for BLAST searches on mouse)
GenBank, http://www.ncbi.nlm.nih.gov/Genbank/ (for the cDNA of *NAV2* [accession number NM_182964], *HTATIP2* [accession number NM_006410], *PRMT3* [accession number XM_058460], *SLC6A5* [accession number NM_004211], *NELL1* [accession number NM_006157], *SLC17A6* [accession number NM_020346], *FANCF* [accession number NM_022725], *GAS2* [accession number NM_005256], and *GDD1* [accession numbers AL833271 and AB125267] and the GDD1 ortholog amino acid sequences of mouse [accession number AB125740], zebrafish [accession number CAD43466], fruit fly [accession number NP_648535], and mosquito [accession number XP_311470])
MOTIF, http://motif.genome.ad.jp/
Online Mendelian Inheritance in Man (OMIM), http://www.ncbi.nlm.nih.gov/Omim/ (for osteogenesis imperfecta with unusual skeletal lesions)
PSORT II, http://psort.ims.u-tokyo.ac.jp/
TMpred, http://www.ch.embnet.org/software/TMPRED_form.html
UCSC Genome Bioinformatics, http://genome.ucsc.edu (for public genome assembly and BLAST alignments)

References

Akasaka Y, Nakajima T, Koyama K, Furuya K, Mitsuka Y (1969) Familial cases of new systemic bone disease, hereditary gnatho-diaphyseal sclerosis. Nippon Seikeigeka Gakkai Zasshi 43:381–394 (In Japanese)

Colavita N, Kozlowski K, La Vecchia G, Fileni A, Ricci R (1984) Calvarial doughnut lesions with osteoporosis, multiple fractures, dentinogenesis imperfecta and tumorous changes in the jaws: report of a case. Australas Radiol 28: 226–231

Hahn TJ, Westbrook SL, Sullivan TL, Goodman WG, Halstead LR (1988) Glucose transport in osteoblast-enriched bone explants: characterization and insulin regulation. J Bone Miner Res 3:359–365

Kumagai H, Sacktor B, Filburn CR (1991) Purinergic regulation of cytosolic calcium and phosphoinositide metabolism in rat osteoblast-like osteosarcoma cells. J Bone Miner Res 6:697–707

Levin LS, Wright JM, Byrd DL, Greenway G, Dorst JP, Irani RN, Pyeritz RE, Young RJ, Laspia CL (1985) Osteogenesis imperfecta with unusual skeletal lesions: report of three families. Am J Med Genet 21:257–269

Ljunggren O, Johansson H, Ljunghall S, Fredholm BB, Lerner UH (1991) Bradykinin induces formation of inositol phosphates and causes an increase in cytoplasmic Ca2+ in the osteoblastic cell line MC3T3-E1. J Bone Miner Res 6:443–452

Ma Y, Hendershot LM (2001) The unfolding tale of the unfolded protein response. Cell 107:827–830

Meszaros JG, Karin HJ (1995) Inhibitors of ER Ca(2+)-ATPase activity deplete the ATP- and thrombin-sensitive Ca2+ pool in UMR 106-01 osteosarcoma cells. J Bone Miner Res 10:704–710

Neville BW, Albenesius RJ (1986) The prevalence of benign fibro-osseous lesions of periodontal ligament origin in black women: a radiographic survey. Oral Surg Oral Med Oral Pathol 62:340–344

Nishimura G, Haga N, Ikeuchi S, Yamaguchi T, Aoki K, Yamato M (1996) Fragile bone syndrome associated with craniognathic fibro-osseous lesions and abnormal modeling of the tubular bones: report of two cases and review of the literature. Skeletal Radiol 25:717–722

Pettit EJ, Fay FS (1998) Cytosolic free calcium and the cytoskeleton in the control of leukocyte chemotaxis. Physiol Rev 78:949–967

Riminucci M, Collins MT, Corsi A, Boyde A, Murphey MD, Wientroub S, Kuznetsov SA, Cherman N, Robey PG, Bianco P (2001) Gnathodiaphyseal dysplasia: a syndrome of fibro-osseous lesions of jawbones, bone fragility, and long bone bowing. J Bone Miner Res 16:1710–1718

Smith MJ, Koch GL (1989) Multiple zones in the sequence of calreticulin (CRP55, calregulin, HACBP), a major calcium binding ER/SR protein. EMBO J 8:3581–3586

Teasdale RD, Jackson MR (1996) Signal-mediated sorting of membrane proteins between the endoplasmic reticulum and the Golgi apparatus. Annu Rev Cell Dev Biol 12:27–54

Tsutsumi S, Kamata N, Maruoka Y, Ando M, Tezuka O, Enomoto S, Omura K, Nagayama M, Kudo E, Moritani M, Yamaoka T, Itakura M (2003) Autosomal dominant gnathodiaphyseal dysplasia maps to chromosome 11p14.3-15.1. J Bone Miner Res 18:413–418

Waldron CA, Giansanti JS (1973) Benign fibro-osseous lesions of the jaws: a clinical-radiologic-histologic review of sixty-five cases. II. Benign fibro-osseous lesions of periodontal ligament origin. Oral Surg Oral Med Oral Pathol 35:340–350